Absolute Cross Sections of the Reactions $Na^{23}(n,p)Ne^{23}$ and $Na^{23}(n,\alpha)F^{20}$[†]

CLAUDE F. WILLIAMSON*

Department of Physics, The University of Texas, Austin, Texas

(Received February 3, 1961)

The absolute cross sections for the competing reactions $Na^{23}(n,p)Ne^{23}$ and $Na^{23}(n,\alpha)F^{20}$ have been measured over the energy range 4 to 19 Mev by the activation method using neutrons from the $H^2(d,n)He^3$, $N^{14}(d,n)O^{15}$, $C^{14}(d,n)N^{15}$, and $H^3(d,n)He^4$ reactions. The excitation curves thus obtained are compared with theoretical results based upon the statistical theory. A fair fit is obtained for the (n,p) reaction, but serious discrepancies exist between the measured and calculated (n,α) cross sections.

INTRODUCTION

THE existence of two different short-lived activities arising from fast neutron bombardment of sodium has been known for many years.[1-4] These were recognized to be from (n,p) and (n,α) reactions in Na^{23}. However, until about three years ago only isolated measurements of the absolute cross sections had been made.[5,6] The first detailed measurement of the $Na^{23}(n,p)Ne^{23}$ excitation curve was reported by Bostrom *et al.* in 1957.[7] This was followed in 1958 by a measurement over a more extended energy range by Williamson *et al.*[8] Unfortunately, the latter contained a numerical error. Also, the $N^{14}(d,n)O^{15}$ cross sections of Weil and Jones[9] which were used in computing the (n,p) cross sections have subsequently been shown to be in error by as much as a factor of 2 at some energies.[10] These errors have been corrected in the present paper, and the energy range covered has been greatly extended by the use of the $C^{14}(d,n)N^{15}$ and $H^3(d,n)He^4$ reactions as neutron sources. In addition, measurements of the absolute cross sections of the $Na^{23}(n,\alpha)F^{20}$ reaction have been made.

TARGETS

Neutrons for exciting the observed reactions were produced by bombarding the appropriate targets with a deuteron beam from the University of Texas electrostatic generator. The range of deuteron beam energies used was 0.6 to 3.2 Mev, with a spread of ± 7 kev. The energy was measured by a magnetic resonance gaussmeter whose sensing element was placed in the field of the analyzing magnet. This apparatus was calibrated

with the $Li^7(p,n)Be^7$ threshold at 1.8814 Mev, and the energy scale is believed to be known to ± 4 kev over the energy range used.

Gas targets 2 and 4 cm deep were used for deuterium and nitrogen bombardment, the gas being separated from the vacuum system by thin nickel foils. The C^{14} target consisted of a solid carbon target of 0.178 mg/cm² thickness enriched 10% in C^{14}. The tritium target was a Zr-T target whose thickness was 0.486 mg/cm².

The pressure of the gas targets was measured either by a U-tube open-end mercury manometer or by a $\frac{1}{4}$% accurate Bourdon gauge. Nickel windows of known area were weighed on a precision microbalance before being installed in the target system. Thicknesses of the windows ranged from 0.6 to 2.1 mg/cm².

The C^{14} solid target was prepared by polymerization of 10% C^{14} enriched acetylene on a 10 mil tantalum backing. Its thickness was measured by two methods.[11] The first consisted of observing the width at half-maximum of the $C^{13}(p,\gamma)N^{14}$ resonance at 1.76-Mev proton energy. The second consisted of observing the $C^{12}(d,n)N^{13}$ delayed activity yield from the target in question and comparing this yield to the N^{13} yield from a normal carbon target whose thickness had been accurately determined by weighing. The two methods yielded thicknesses that differed by only 7%. This was within the experimental error of ± 10%.

The Zr-T target was supplied by the isotopes division of the Oak Ridge National Laboratory. The thickness of this target was checked by observing the $H^3(p,n)He^3$ yield with a calibrated "long counter." By assuming a one-to-one ratio of tritium to zirconium, a value of the thickness was obtained that differed from the value supplied by Oak Ridge by less than the estimated experimental error of ± 15% for the measurement.

MEASUREMENT OF THE NEUTRON YIELD

It was felt that it would be desirable not to have to depend entirely on the calculation of neutron flux. Absolute measurements of the yield were therefore made for each of the neutron sources used. The flux of neutrons from the $H^2(d,n)He^3$ reaction was measured by a standard "long counter" which had been calibrated

† Assisted by the U. S. Atomic Energy Commission.
* Now at Le Centre d'Études Nucléaires de Saclay, Gif-sur-Yvette, Seine-et-Oise, France.
¹ E. Fermi *et al.*, Proc. Roy. Soc. (London) **A146**, 483 (1934).
² E. Amaldi *et al.*, Proc. Roy. Soc. (London) **A149**, 522 (1935).
³ M. E. Nahmias and R. J. Walen, Compt. rend. **203**, 71 (1936).
⁴ A. Polessitsky, Physik Z. Sowjetunion **12**, 339 (1937).
⁵ J. V. Jelley and E. B. Paul, Proc. Phys. Soc. (London) **A63**, 112 (1950).
⁶ E. B. Paul and R. L. Clarke, Can. J. Phys. **31**, 267 (1953).
⁷ N. A. Bostrom, R. G. Moore, and I. L. Morgan, Bull. Am. Phys. Soc. **2**, 104 (1957).
⁸ C. F. Williamson, E. L. Hudspeth, I. L. Morgan, and R. G. Moore, Phys. Rev. **110**, 139 (1958).
⁹ J. L. Weil and K. W. Jones, Phys. Rev. **112**, 1975 (1958).
¹⁰ T. Retz-Schmidt and J. M. Weil, Phys. Rev. **119**, 1079 (1960).

¹¹ C. E. Brient, Master's thesis, The University of Texas, Austin, Texas, 1960 (unpublished).
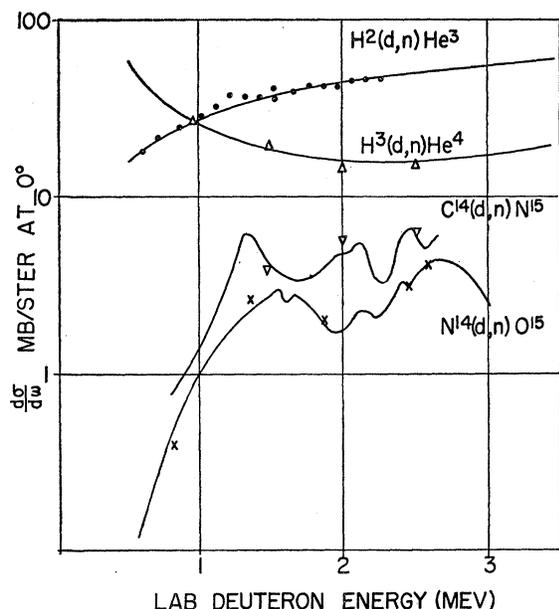
FIG. 1. Cross sections for the neutron-producing reactions used in this experiment (references 10, 11, 14, and 15). The symbol designations for the absolute yield measurements are as follows: ●—$H^2(d,n)He^3$ neutrons, △—$H^3(d,n)He^4$ neutrons, ▽—$C^{14}(d,n)N^{15}$ neutrons, ✕—$N^{14}(d,n)O^{15}$ neutrons.

with a Ra-Be source of known strength. The yields from the $N^{14}(d,n)O^{15}$ and $C^{14}(d,n)N^{15}$ sources were measured by observing the proton recoil spectrum in a 3 mm✕3 mm cylinder of plastic scintillator. The $H^3(d,n)He^4$ yield was measured by observing the recoil proton spectra produced in a 1 in.✕1 in. stilbene crystal with a pulse shape discrimination spectrometer.[12] All proton recoil spectra were displayed on a 100-channel analyzer and analyzed according to the methods of Swartz and Owen.[13] The results of the absolute flux measurements are shown in Fig. 1, along with the published excitation curves for the various neutron-producing reactions.[10,11,14,15]

Other workers have reported observing a reduction in neutron yield per unit charge with increasing beam current,[16,17] and have attributed this to a local reduction in gas density due to heating of the gas and foil by the beam. In an attempt to measure the magnitude of this effect the (n,p) activity per unit charge was observed after bombardments with various beam currents. The beam was also artificially decreased by defocusing. No significant effect on the (n,p) yield was

observed in the range of beam currents (0.2 to 1 μa) employed in this experiment. It is therefore concluded that the error from this source is probably less than 5%.

The contribution from room background neutrons was measured by the inverse square method. This contribution was also found to be less than 5%.

EXPERIMENTAL ARRANGEMENT

Figure 2 shows schematically the experimental arrangement used in this work. The sodium sample which was activated was in the form of a $1\frac{1}{2}$ in.✕$1\frac{1}{2}$ in. NaI(Tl) scintillation crystal which was mounted on a DuMont 6292 photomultiplier. The crystal thus served as both target and 4π counter. The photomultiplier base was mounted on an arm which could be swung away from the Van de Graaff target to a distance of about 6 ft after irradiation to avoid the strong background following the deuteron bombardment.

The face of the crystal was 2 to 4 in. from the face of the target. This distance was measured and frequently checked with a pair of machinist's calipers. The thickness of the target mounting and the thickness of the reflective material around the crystal were also taken into account in calculating the solid angle.

The target itself was insulated and electron emission was suppressed. It connected to a "leaky integrator" of the type reported by Snowdon.[18] The value of the capacitors (polystyrene type) was known to 1% accuracy, and the time constant of the resistance-capacitance network was adjusted to be equal to the mean life of the activity under observation. The half-lives used were: F^{20}—10.7 sec,[18] Ne^{23}—37.6 sec.[19] The voltage across the integrator was measured by a calibrated
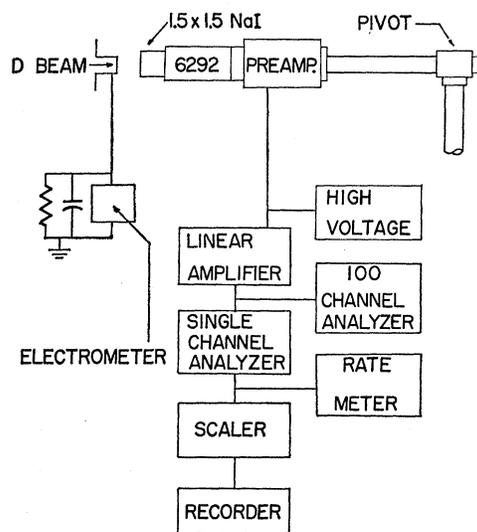
FIG. 2. Schematic diagram of equipment used in this experiment.

[12] R. B. Owen, L'Électronique Nucléaire (Kärtner Ring, Vienna, 1959), p. 27.

[13] C. D. Swartz and G. E. Owen, Fast Neutron Physics (Interscience Publishers, Ltd., London, 1960), Part I, p. 211.

[14] Los Alamos Publication LA-2014, 27, 1957 (unpublished).

[15] S. J. Bame, Jr., and J. E. Perry, Jr., Phys. Rev. 107, 1616 (1957).

[16] I. L. Morgan, The Texas Nuclear Corporation, Austin, Texas (private communication).

[17] J. H. Coon, Fast Neutron Physics (Interscience Publishers, Ltd., London, 1960), Part I, p. 708.

[18] S. C. Snowdon, Phys. Rev. 78, 299 (1950).

[19] J. R. Pennig and F. H. Schmidt, Phys. Rev. 105, 647 (1957).

Keithley model 210 electrometer with an input impedance of at least 10^{14} ohms and a rated accuracy of 2% full scale.

The electronic equipment consisted of a standard scintillation spectrometer with the exception of the Sanborn model 107 recorder. The register drive pulse of the scaler was of sufficient amplitude and duration to actuate the recorder pen, so that the activity can be recorded on the recorder tape scaled down by a factor of 8 or 64. These tapes were then analyzed at leisure.

METHOD OF TAKING DATA

In order to avoid the high background associated with a low bias setting, the integral bias of the pulse height analyzer was set so that about one-half of the β spectrum of the activity being counted was accepted. This resulted in a factor of 100 decrease in background over a low bias setting.

The energy calibration of the spectrometer was determined by observing the differential bias settings corresponding to the γ-ray peaks from Cs^{137}, Na^{22}, and Co^{60}. Routine checks and adjustments of the calibration were made at least every hour during the course of the experiment using the peaks from Na^{22} as standards. A ratemeter greatly facilitated finding the exact positions of these peaks.

It is possible to calculate from the Fermi theory the fraction of the β spectrum accepted at a given integral bias setting. This has been done in Fig. 3 for Ne^{23} β rays (67% of which have 4.4-Mev end-point energy and 32% of which have 4.0-Mev end-point energy and are accompanied by a 0.43-Mev γ ray) and is compared with experiment. The fact that the experimental curve falls below the theoretical curve at higher bias energies can probably be attributed to crystal edge effects. In the calculations, the experimental curve was used.

The yield from F^{20} (5.42-Mev end-point energy accompanied by a 1.62-Mev γ ray) was never great enough to allow an accurate experimental determination of the integral bias curve. The higher average energy of the β rays from this isotope would tend to enhance the edge effects; however, the coincidences between the γ rays and β rays would tend to cancel the edge effects. Thus, the calculated fraction accepted was used in the (n,α) cross section calculations. This, however, introduces a slight added uncertainty of about 6% in the (n,α) calculations.

EXPERIMENTAL RESULTS

Figure 4 shows the cross sections measured with neutrons from the H$^2(d,n)$He^3 and N$^{14}(d,n)$O^{15} sources. The neutron energy resolution for the (n,p) reaction in this energy range was 20 to 40 kev. There is reasonably good agreement for the (n,p) reaction in the region where the neutrons from the deuterium and nitrogen reactions have corresponding energies. This furnishes
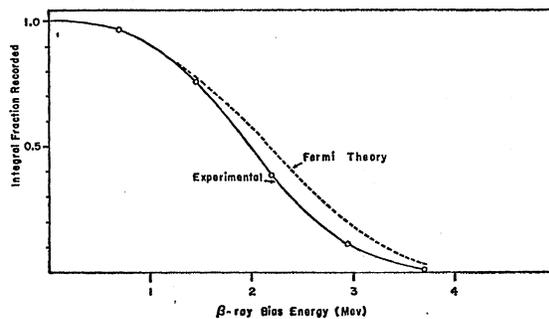
FIG. 3. Integral bias counting curve for Ne^{23}. The theoretical curve from the Fermi theory is shown for comparison.

an independent verification over a short energy range of the N$^{14}(d,n)$O^{15} cross sections measured by Retz-Schmidt and Weil.[10]

The (n,α) reaction was unobservable below a neutron energy of 6 Mev. Below 8 Mev the energy resolution of the (n,α) cross sections had to be sacrificed in favor of a thick nitrogen target in order to obtain a usable activity. The neutron energy spread varied from 130 kev at the lower energies to 70 kev at the higher energies.

Figure 5 shows the cross sections in the region from 8 to 20 Mev. The energy resolution for the points taken with C$^{14}(d,n)$N^{15} neutrons varied from about 40 kev at the lower energies to about 30 kev at the higher energies. However, data points were taken every 50 kev because the detailed structure of the C$^{14}(d,n)$N^{15} excitation curve is not yet known with enough precision to justify observations in smaller energy increments.

Above 16 Mev the cross sections of both the (n,p) and (n,α) reactions are decreasing with increasing energy. Since detailed structure would not be expected at this high excitation, only enough points were taken to establish the trend of the curve.

In all cases it was necessary to correct for the energy loss in the various targets. This was done by calculating the stopping powers for the various substances using the Bethe[20] formula. The parameters in this equation were adjusted to give the best possible fit to the small amount of experimental stopping power data which is available.

The neutron energies at the mean angle subtended by the counter were taken from published tables[21] which are corrected for relativistic effects. However, no published energy tables are available for the N$^{14}(d,n)$O^{15} and C$^{14}(d,n)$N^{15} reactions. These were calculated from the nonrelativistic energy-angle formula using Q values of 5.073 Mev for the nitrogen neutrons and 7.987 Mev for the carbon neutrons.[22]

[20] M. S. Livingston and H. A. Bethe, Revs. Modern Phys. 9, 245 (1937); see p. 263.

[21] L. Blumberg and S. I. Schlesinger, Los Alamos Scientific Laboratory Publication AECU-3118 (unpublished).

[22] F. Ajzenberg-Selove and T. Lauritsen, Nuclear Phys. 11, 5 (1959).
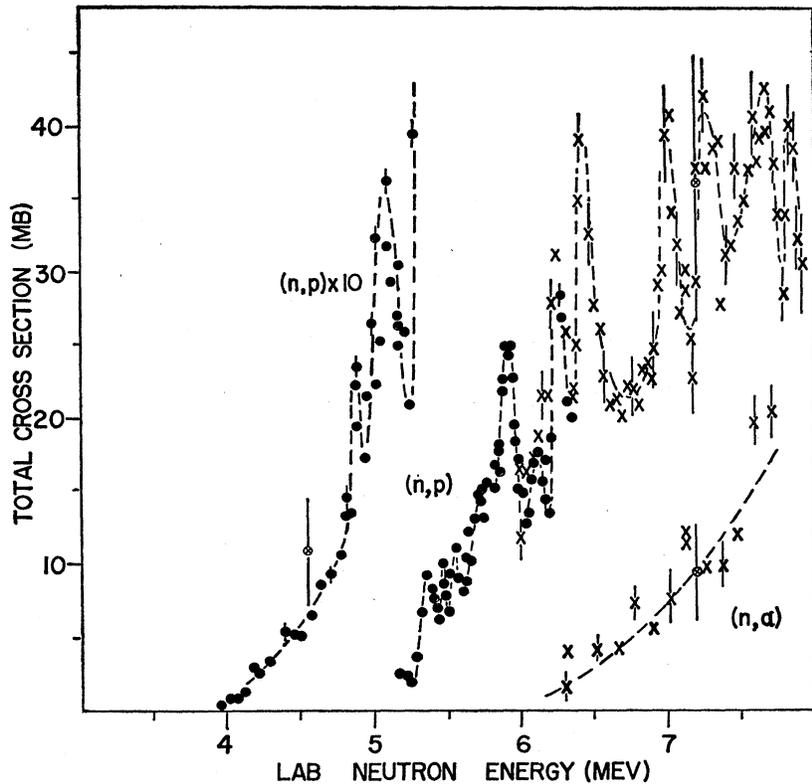
FIG. 4. Cross sections for the reactions $Na^{23}(n,p)Ne^{23}$ and $Na^{23}(n,\alpha)F^{20}$ for laboratory energies less than 8 Mev. Symbol designations are as follows: ●— points taken with $H^2(d,n)He^3$ neutrons; ✕—points taken with $N^{14}(d,n)O^{15}$ neutrons; ⊗—points taken by Jelley and Paul (reference 5). Statistical errors only are shown for the present work, total errors for previous work.

It is estimated that the uncertainty in neutron energy was ±15 kev over the entire range used.

THEORY

The statistical approach to the explanation of nuclear reactions was first put on a consistent theoretical basis by Weisskopf and Ewing.[23] The theory has essentially remained in its original form, the main work being concentrated on obtaining better formulas for level densities and compound nucleus cross sections.

According to the Weisskopf-Ewing theory the cross section $\sigma(a,b)$ for a reaction in which particle a is absorbed to form a compound nucleus and particle b is emitted and can be written

$$\sigma(a,b)=\sigma_c(a)(\Gamma_b/\sum_i\Gamma_i),\qquad(1)$$

where the Γ's are the relative reaction widths and the sum in the denominator extends over all available emission channels.

The Γ's can be written as

$$\Gamma_b=KM_b\nu_b\int_0^{\epsilon_b^{max}}\epsilon_b\sigma_b(\epsilon_b)\omega(U)d\epsilon_b,\qquad(2)$$

where K is a constant; M_b is the mass of the emitted particle; ν is one for emitted particles with nonzero spin and is one-half for emitted particles with zero

[23] V. Weisskopf and D. Ewing, Phys. Rev. 57, 472 (1940).

spin; ϵ_b is the energy of the emitted particle; $\omega(U)$ is the density of states of the residual nucleus at a level of excitation U remaining after emission of particle b; and $\sigma_b(\epsilon_b)$ is the cross section for compound nucleus formation by the inverse reaction.

There have been many attempts to evaluate the density-of-states function.[24–28] One of the most recent and most successful attempts was performed by Newton.[29] He obtains a level density formula for states of zero spin of

$$\omega(U)=\text{const}\frac{\exp[2(aU)^{\frac{1}{2}}]}{A^{5/3}(2j_p+1)^{\frac{1}{2}}(2j_n+1)^{\frac{1}{2}}[2U+3(U/A)^{\frac{1}{2}}]^2},\qquad(3)$$

where $a=0.062(j_p+j_n+1)A^{\frac{2}{3}}$, and j_n and j_p are the spins of the last neutron and last proton, respectively. A is the nuclear mass number and all symbols are as above.

These equations as they stand do not take into account the symmetry effect. It is well known that odd-odd nuclei have a higher density of states than odd-A nuclei, which in turn have a higher density of states than even-even nuclei. This is often taken into

[24] H. A. Bethe, Revs. Modern Phys. 9, 79 (1937).
[25] C. Van Lier and G. Uhlenbeck, Physica 4, 531 (1937).
[26] J. Lang and R. LeCouteur, Proc. Phys. Soc. (London) A67, 586 (1954).
[27] H. Hurwitz and H. A. Bethe, Phys. Rev. 81, 898 (1951).
[28] G. Brown and H. Muirhead, Phil. Mag. 2, 473 (1957).
[29] T. D. Newton, Can. J. Phys. 34, 804 (1956).

FIG. 5. Cross sections for the reactions Na²³(n,p)Ne²³ and Na²³(n,α)F²⁰ in the laboratory neutron energy range 8 to 20 Mev. Symbol designations are as follows: ●—measurements of the (n,p) cross sections; ✕—measurements of the (n,α) cross section; ⊗—measurement of the (n,p) cross section by Paul and Clarke (reference 6).
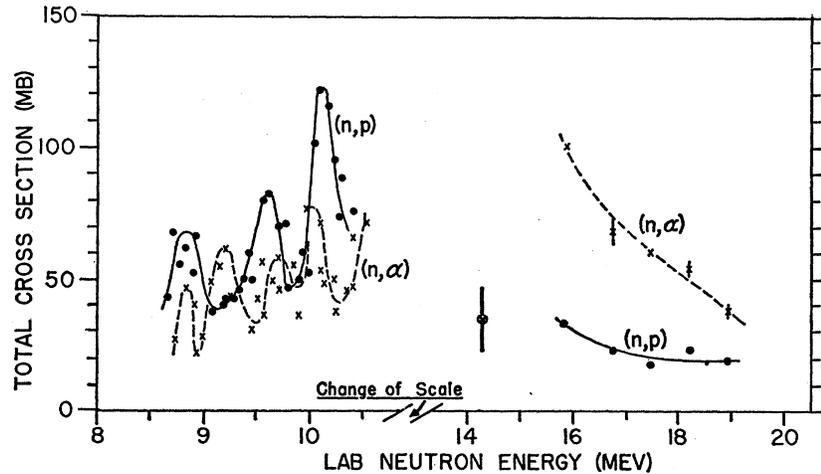
account by multiplying the density of states by constant factors which have been determined empirically.

A more satisfactory method from a theoretical standpoint is to assume that neighboring nuclei have similar level density structures, but that the density of states for odd-A and odd-odd nuclei begins to rise from a reference line below the ground-state energy. In the computations herein it was assumed that this reference line was the ground state of the nearest even-even nucleus.

To get the effective energy of excitation for calculating the density of states of odd-A nuclei, the pairing energy δ was added to the excitation energy of the residual nucleus. For odd-odd residual nuclei, 2δ was added to the final excitation energy. The value of δ used was that of Green[30] which is given in Mev by

$$\delta = 10A^{-\frac{1}{2}},$$

where A is again the mass number. The density-of-states function then becomes

$$\omega(U) = \omega(\epsilon_b^{max} - \epsilon_b + n\delta),$$

where n is 0, 1, or 2 depending on whether the residual nucleus is even-even, odd-A, or odd-odd, respectively.

Values of $\sigma_b(\epsilon_b)$ for charged particles were taken from the tables of Shapiro,[31] and values of $\sigma_c(a)$ for neutrons were taken from Blatt and Weisskopf.[32] In all cases a radius constant of 1.5 fermis was assumed.

In order to obtain the (a,b) cross section from Eq. (1), one must integrate as indicated in Eq. (2). This was done in practice by plotting the spectra of all emitted particles at a given bombarding energy and integrating these spectra numerically. This yielded the Γ_b which could then be used in Eq. (1) to calculate the competing cross sections.

This experiment covered such a large span of bombarding energies that over much of this range second particle emission was energetically possible. Corrections for second particle emission were made in these calculations.

The cross sections for the various reactions arising from neutron bombardment of Na²³ have been calculated. Table I gives the Q values used in these calcula-

[30] A. E. S. Green, Nuclear Physics (McGraw-Hill Book Company, Inc., New York, 1955), p. 250.
[31] M. M. Shapiro, Phys. Rev. 90, 171 (1953).
[32] J. M. Blatt and V. F. Weisskopf, Theoretical Nuclear Physics (John Wiley & Sons, New York, 1956), p. 348.
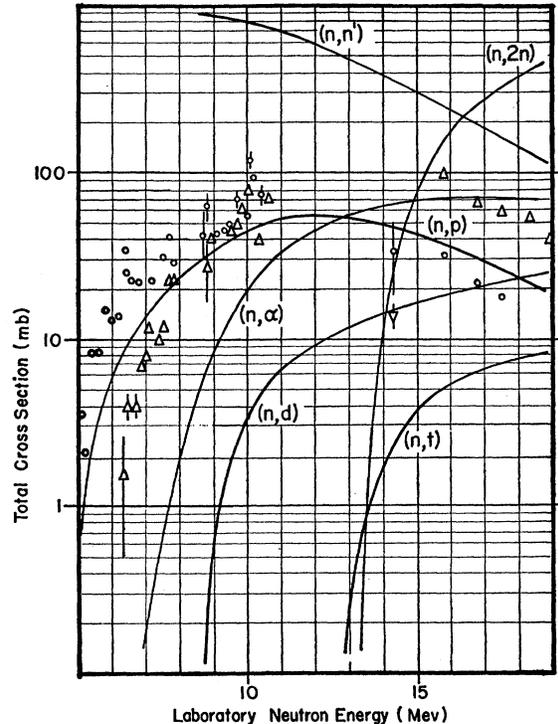
FIG. 6. Cross sections for neutron-induced reactions on Na²³, calculated on the basis of the statistical theory as described in the text. Symbol designations are as follows: ○—typical (n,p) data points; △—typical (n,α) data points; ▽—(n,2n) measurement by Paul and Clarke (reference 6).

TABLE I. Q values[a] for neutron-induced reactions in Na^{23} in the energy range 0 to 20 Mev.

Reaction	Q value (Mev)	Delayed activity
$Na^{23}(n,p)Ne^{23}$	-3.603 ± 0.015	37.6 sec
$Na^{23}(n,\alpha)F^{20}$	-3.887 ± 0.014	11.7 sec
$Na^{23}(n,d)Ne^{22}$	-6.569 ± 0.015	stable
$Na^{23}(n,np)Ne^{22}$	-8.795 ± 0.015	stable
$Na^{23}(n,t)Ne^{21}$	-10.379 ± 0.014	stable
$Na^{23}(n,n\alpha)F^{19}$	-10.493 ± 0.016	unknown
$Na^{23}(n,2n)Na^{22}$	-12.419 ± 0.016	2.60 yr
$Na^{23}(n,p\alpha)O^{19}$	-14.498 ± 0.016	29.4 sec
$Na^{23}(n,He^3)F^{21}$	-16.387 ± 0.035	unknown
$Na^{23}(n,nd)Ne^{21}$	-16.935 ± 0.015	stable
$Na^{23}(n,2np)Ne^{21}$	-19.161 ± 0.035	stable

[a] See reference 22.

tions, and Fig. 6 shows theoretical cross sections with typical data points to illustrate the fit.

DISCUSSION

With one exception the present data agree within experimental limits with previous work. Table II summarizes both previous measurements and the present work. There is agreement except for the (n,α) point taken by Jelley and Paul[5] with $Be^9(d,n)B^{10}$ neutrons. In the present experiment no (n,α) activity was observed below a neutron energy of 6 Mev. The point taken by Paul and Clarke[6] with $H^3(d,n)He^4$ neutrons appears to agree fairly well with the extrapolated trend of the present curve.

In the present work the $H^2(d,n)He^3$ and $H^3(d,n)He^4$ reactions are monoergic; however, this is not true for the neutrons from the other two reactions used. Fortunately, in the energy range covered, the neutron group producing the first excited state in O^{15} is never energetic enough to excite either of the reactions studied. Thus no correction is necessary to the cross sections measured with $N^{14}(d,n)O^{15}$ neutrons.

The situation is somewhat different in the case of the $C^{14}(d,n)N^{15}$ neutrons. At the highest bombarding energy the first excited state group from this reaction can excite the (n,p) reaction in an energy region where

the cross section of the latter is about 3 to 6 mb. Thus, it is not unlikely that there is some contribution from the first excited state group. This may cause the apparent (n,p) cross section to be larger than the true cross section. It will be necessary to have more information concerning the energy spectrum of the neutrons emitted in this reaction before any correction can be made.

The absolute errors assigned to the data were compounded from estimates of individual experimental errors. These absolute errors are listed according to the neutron source used for the excitation. They are as follows: $H^2(d,n)He^3$—16%; $N^{14}(d,n)O^{15}$—24%; $C^{14}(d,n)N^{15}$—33%; $H^3(d,n)He^4$—19%.

It appears from Fig. 6 that the statistical theory gives a fair account of the (n,p) reaction except in the energy region below the top of the Coulomb barrier. The fit for the (n,α) reaction is poor and the shape of the theoretical curve appears to be significantly in error.

These discrepancies could be qualitatively explained by assuming that many more low-energy charged particles are emitted than the present theory predicts. A possible mechanism for this is suggested in a paper by Németh.[33] According to calculations by the latter, the penetrability of the Coulomb barrier of an excited nucleus may be significantly greater than expected owing to an effective lowering of the barrier by excitation. It is impossible to say at the present time if this is responsible for the observed discrepancies because no numerical calculations that take this effect into account have been made.

The rather prominent resonance structure observed in the (n,p) reaction for neutron energies below 10.5 Mev is probably caused by the energy level structure in the compound nucleus Na^{24}. Since the density of resonances on the present excitation curve is less than the observed density of levels at the neutron binding energy, it appears likely that the observed resonance structure is due to groupings of unresolved levels in Na^{24}.

ACKNOWLEDGMENTS

TABLE II. Summary of previous work and comparison with the present work on neutron activation of Na^{23}.

Workers	Neutron energy (Mev)	$\sigma(n,\alpha)$ (mb)	$\sigma(n,p)$ (mb)	$\sigma(n,2n)$ (mb)	Neutron source
Jelley and Paul[a]	4.55	1.12	1.08	$\cdots$	$Be^9(d,n)B^{10}$
Present work	4.55	<0.1	0.52	$\cdots$	$H^2(d,n)He^3$
Jelley and Paul[a]	7.20	9.51	36.4	$\cdots$	$B^{10}(d,n)C^{11}$
Present work	7.20	9.6	34.0	$\cdots$	$N^{14}(d,n)O^{15}$
Jelley and Paul[a]	$\cdots$	118.7	80.2	$\cdots$	$Li^7(d,n)Be^8$
Paul and Clarke[b]	14.3	$\cdots$	34	14	$H^3(d,n)He^4$

[a] Reference 5.
[b] Reference 6.

[33] J. Németh, Nuclear Phys. 16, 331 (1960).